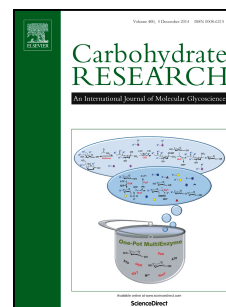


Accepted Manuscript

Synthesis and use of 6,6,6-trifluoro-L-fucose to block core-fucosylation in hybridoma cell lines

Nicole C. McKenzie, Nichollas E. Scott, Alan John, Jonathan M. White, Ethan D. Goddard-Borger



PII: S0008-6215(18)30238-6

DOI: [10.1016/j.carres.2018.05.008](https://doi.org/10.1016/j.carres.2018.05.008)

Reference: CAR 7567

To appear in: *Carbohydrate Research*

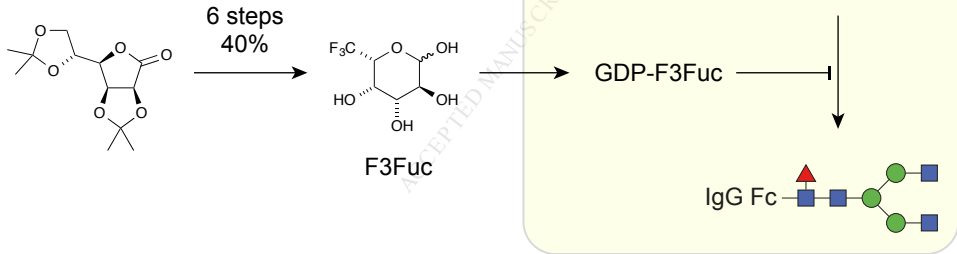
Received Date: 17 April 2018

Revised Date: 17 May 2018

Accepted Date: 19 May 2018

Please cite this article as: N.C. McKenzie, N.E. Scott, A. John, J.M. White, E.D. Goddard-Borger, Synthesis and use of 6,6,6-trifluoro-L-fucose to block core-fucosylation in hybridoma cell lines, *Carbohydrate Research* (2018), doi: 10.1016/j.carres.2018.05.008.

This is a PDF file of an unedited manuscript that has been accepted for publication. As a service to our customers we are providing this early version of the manuscript. The manuscript will undergo copyediting, typesetting, and review of the resulting proof before it is published in its final form. Please note that during the production process errors may be discovered which could affect the content, and all legal disclaimers that apply to the journal pertain.



Synthesis and use of 6,6,6-trifluoro-L-fucose to block core-fucosylation in hybridoma cell lines

Nicole C. McKenzie^{1,2}, Nichollas E. Scott³, Alan John^{1,2}, Jonathan M. White^{4,5}, Ethan D. Goddard-Borger^{1,2*}

1. ACRF Chemical Biology Division, The Walter and Eliza Hall Institute of Medical Research, Parkville, VIC, 3052, Australia

2. Department of Medical Biology, University of Melbourne, Parkville, VIC, 3010, Australia

3. Department of Microbiology and Immunology, University of Melbourne at the Peter Doherty Institute for Infection and Immunity, Parkville, VIC, 3010, Australia

4. School of Chemistry, University of Melbourne, Parkville, VIC, 3010, Australia

5. Bio21 Molecular Science and Biotechnology Institute, University of Melbourne, Parkville, VIC 3010, Australia

* Corresponding author. E-mail: goddard-borger.e@wehi.edu.au

Abstract

Many monoclonal antibodies (mAbs) used in cancer immunotherapy mediate tumour cell lysis by recruiting natural killer (NK) cells; a phenomenon known as antibody-dependent cellular cytotoxicity (ADCC). Eliminating core-fucose from the N-glycans of a mAb enhances its capacity to induce ADCC. As such, inhibitors of fucosylation are highly desirable for the production of mAbs for research and therapeutic use. Herein, we describe a simple synthesis of 6,6,6-trifluoro-L-fucose (F3Fuc), a metabolic inhibitor of fucosylation, and demonstrate the utility of this molecule in the production of low-fucose mAbs from murine hybridoma cell lines.

Keywords

Fucose, enzyme inhibition, monoclonal antibody, hybridoma

1. Introduction

Therapeutic monoclonal antibodies (mAbs) used in oncology adopt many different modes of action, including: inhibition of cell signalling, delivery of a cytotoxic payload, complement-dependent cytotoxicity (CDC) and antibody-dependent cellular cytotoxicity (ADCC).[1] ADCC is the most common mode of action for therapeutic mAbs of the immunoglobulin (Ig) G isotype. To initiate ADCC, a mAb must bind both its cognate antigen on the tumour cell and the Ig gamma Fc receptor

IIIa (FcγRIIIa) on an effector cell. The effector cell, usually a natural killer (NK) cell, then forms a lytic synapse and releases cytotoxic enzymes and pore-forming agents to lyse the tumour cell.[2] The interaction between a therapeutic mAb and FcγRIIIa, which is crucial for this process, involves a conserved complex biantennary N-glycan on Asn297 of the IgG1 heavy chain.[3, 4] While this glycan usually bears α -1,6-linked core-fucose, mAbs without core fucose actually have greater affinity for FcγRIIIa.[4] As a consequence, mAbs lacking core-fucose elicit a more potent ADCC response to low-density antigens,[5] have improved tolerance of FcγRIIIa polymorphisms,[6, 7] and are less prone to competitive inhibition by plasma IgGs.[8] Mogamulizumab, a therapeutic antibody used in the treatment of haematological malignancies, was the first low-fucose mAb approved for use in the clinic.[9]

The improved efficacy of low-fucose mAbs has inspired the development of chemical strategies to disrupt fucosylation in cell lines used for protein production. Two fluorine-substituted fucose-mimics have proven to be useful for inhibiting protein fucosylation in CHO cells lines: 2-deoxy-2-fluoro-L-fucose (2FFuc),[10] and 6,6,6-trifluoro-L-fucose (F3Fuc, **1**).[11] These hijack the fucose salvage pathway to be imported into the cell and converted into the corresponding GDP-fucose mimics.[10, 11] The electron-withdrawing fluorine substituents on these molecules dramatically slows their hydrolysis and glycosyl transfer by fucosyltransferases (FUTs). Accumulation of the GDP-fucose mimics leads to feedback inhibition of the cell's *de novo* pathway for GDP-fucose synthesis, depleting the cell of GDP-fucose, while also providing competitive inhibition of FUTs (Figure 1).[10, 11] Alkynyl fucose derivatives can also inhibit the *de novo* biosynthesis of GDP-fucose,[10, 12] yet they also serve as substrates for some FUTs,[13, 14] making them less desirable than fluorinated fucose analogues for the production of low-fucose proteins.

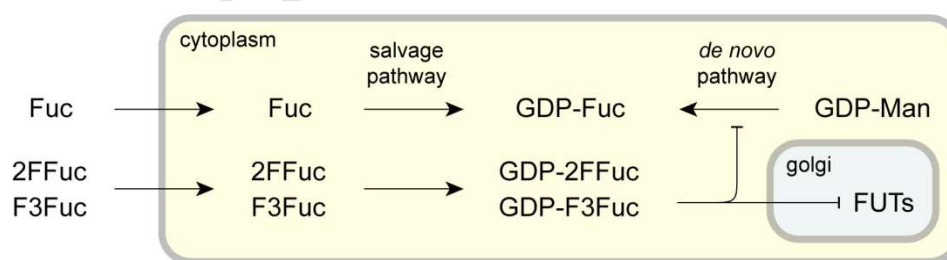


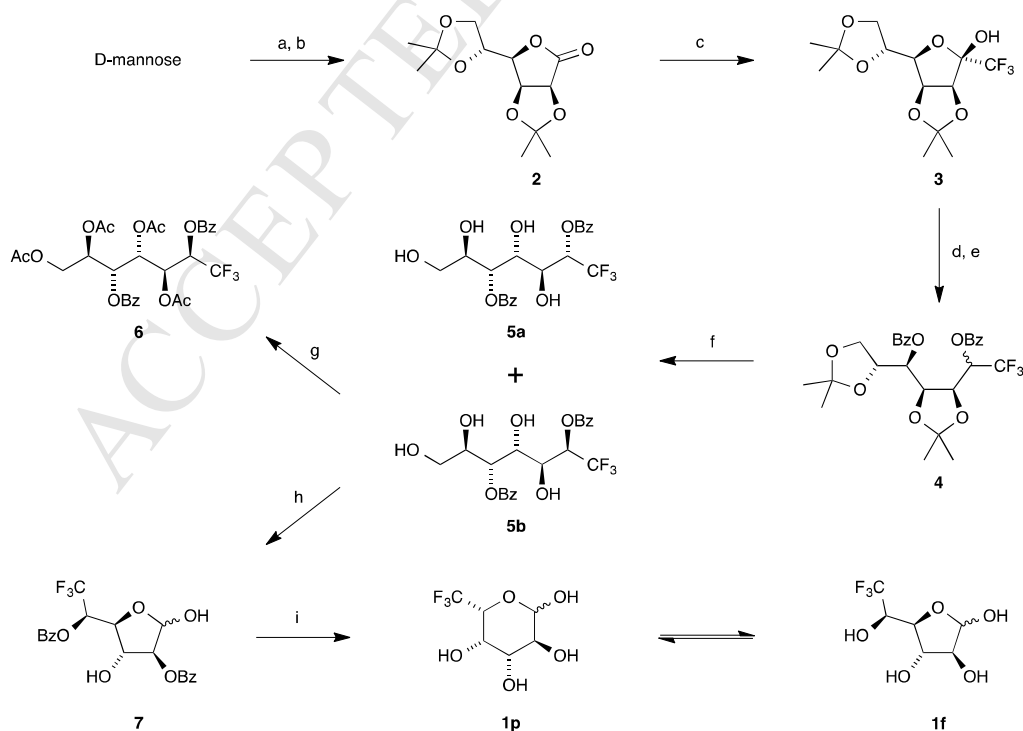
Figure 1. Inhibition of cellular fucosylation by the fucose mimics 2FFuc and F3Fuc.

Here, we present an alternative, high-yielding synthesis of F3Fuc and establish that this molecule can also be used for the production of low-fucose mAbs in murine hybridoma cells lines. This approach provides a convenient means to enhance the ADCC potential of mAbs at the very early stages of therapeutic antibody development.

2. Results and discussion

Two syntheses of F3Fuc (**1**) have been reported.[15, 16] Toyokuni and co-workers first prepared F3Fuc using the rare sugar L-lyxose as a starting material.[15] This approach required stoichiometric quantities of mercuric chloride and the difficult separation of F3Fuc from its epimer 6-deoxy-6,6,6-trifluoro-D-altrose at the final step. A better method was later reported by Caille and co-workers at Amgen, which provides F3Fuc in seven steps from D-arabinose in an 11% overall yield.[16] Nevertheless, the strategy of Petit and co-workers for the synthesis of L-fucose mimics alludes to a shorter route to F3Fuc from D-mannose.[17]

We took the commercially available mannolactone (**2**), which is readily accessible from D-mannose,[18, 19] and treated it with trifluoromethyl(trimethyl)silane (TMSCF₃) and catalytic TBAF to obtain, after workup, a single diastereomer of the lactol (**3**) that was purified directly by recrystallization (Scheme 1). Reduction of the lactol using sodium borohydride followed by benzoylation gave a mixture of diastereomers (**4**) in a ratio of 4:1, as determined by ¹H NMR spectroscopy. Hydrolysis of the acetonides using aqueous trifluoroacetic acid (TFA) provided a complex mixture of products owing to the migration of benzoyl groups to adjacent hydroxyl groups. The use of a weaker acid, aqueous acetic acid, enabled hydrolysis of the acetal groups without causing migration of benzoyl esters to provide the diastereomeric tetraols (**5a**) and (**5b**), which were easily separated by silica gel column chromatography.



Scheme 1. Reagents and conditions: a) I₂, Me₂CO, RT, 16 h, (98%); b) I₂, K₂CO₃, CH₂Cl₂, 40°C, 16 h, (66%); c) TMSCF₃, TBAF, THF, 0°C–RT, 16 h, (95%); d) NaBH₄, EtOH, 0–70°C, 12 h; e) BzCl, DMAP, pyridine, CH₂Cl₂, 0°C–RT, 16 h, (80% over two steps); f) AcOH:H₂O (4:1), 90°C, 2.5 h, (67%); g) Ac₂O, DMAP, pyridine, RT, 16 h, (89%); h) NaIO₄, H₂O, MeOH, 0–12°C, 2 h, (95%); i) NaOMe, MeOH, RT, 2 h, (92%).

To unambiguously determine the relative stereoconfiguration of these diastereomers, the major isomer (**5b**) was converted to the tetraacetate (**6**), which provided crystals suitable for x-ray diffraction studies. This analysis revealed that the major product had the stereochemical configuration required for the synthesis of F3Fuc (**1**) (Figure 2).

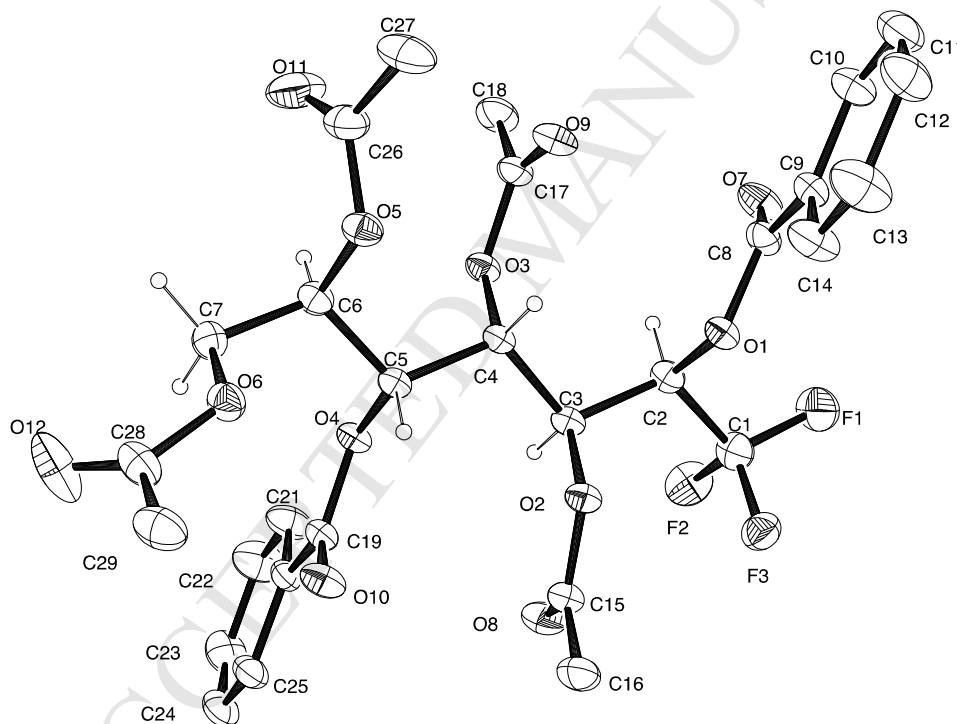


Figure 2. Structural model of tetraacetate **6**, as determined by single crystal x-ray diffraction. Thermal ellipsoids are shown at 50% probability level and implicit hydrogens depicted as small spheres.

A selective periodate-mediated oxidative cleavage of the terminal vicinal diol in (**5b**) proceeded smoothly to give the lactol (**10**). Presumably the less sterically encumbered vicinal diol undergoes oxidative cleavage first to give an aldehyde, which rapidly cyclises to the furanose (**7**),

thereby masking the remaining vicinal diol and preventing further periodate cleavage. The benzoate (7) was submitted to Zemplen transesterification to complete the synthesis, providing F3Fuc (1) in just six steps from the commercially available lactone (2) with an overall yield of 40%.

While, the ability of F3Fuc to inhibit fucosylation has been investigated in CHO cell lines,[16] which are commonly used in industry for the production of therapeutic mAbs, it's activity in murine hybridoma cells lines, which are used for the production of most mAbs in academic research, has not been investigated. To demonstrate the broad utility of F3Fuc, we cultured a monoclonal murine hybridoma cell line in media supplemented with 10 mM F3Fuc, 10 mM L-fucose (negative control) or 10 mM 2FFuc (positive control). The secreted IgG1 isotype mAb was purified from the culture supernatant using protein G immobilised on agarose beads. The isolated mAb was reduced, alkylated and proteolytically digested with trypsin prior to analysis by LC-MS/MS. Semi-quantitation using extracted ion counts provided a good estimate of the degree of core-fucosylation on the mAb expressed under these different conditions (Figures 3 and S1-3). For the L-fucose control, an estimated 80–90% of *N*-glycans at Asn297 of the IgG1 heavy chain possessed core-fucose. This was diminished to 50% in the presence of 10 mM 2FFuc and 4% in the presence of 10 mM F3Fuc (1), revealing that F3Fuc is superior to 2FFuc at inhibiting fucosylation in murine hybridoma cell culture. This may be because F3Fuc retains a hydroxyl group at the C2 position, in contrast to 2FFuc, potentially making it a better substrate for the fucose transporter(s) and enzymes of the fucose salvage pathway that are required for the activity of these metabolic inhibitors of fucosylation. Since F3Fuc provided effective inhibition at 10 mM with no loss in cell viability, we did not explore the use of lower F3Fuc concentrations. However, to economise the use of F3Fuc in large scale protein production optimisation will likely be required, bearing in mind that subtle variations in culture techniques can dramatically impact protein glycosylation.[20]

3. Conclusion

The short and high-yielding route to F3Fuc described here provides easy access to an effective inhibitor of cellular fucosylation. F3Fuc proved to be superior to 2FFuc at inhibiting core fucosylation of mAbs in murine hybridoma cell lines, making it a valuable tool for generating the low-fucose mAbs that early-stage ADCC research programs require.

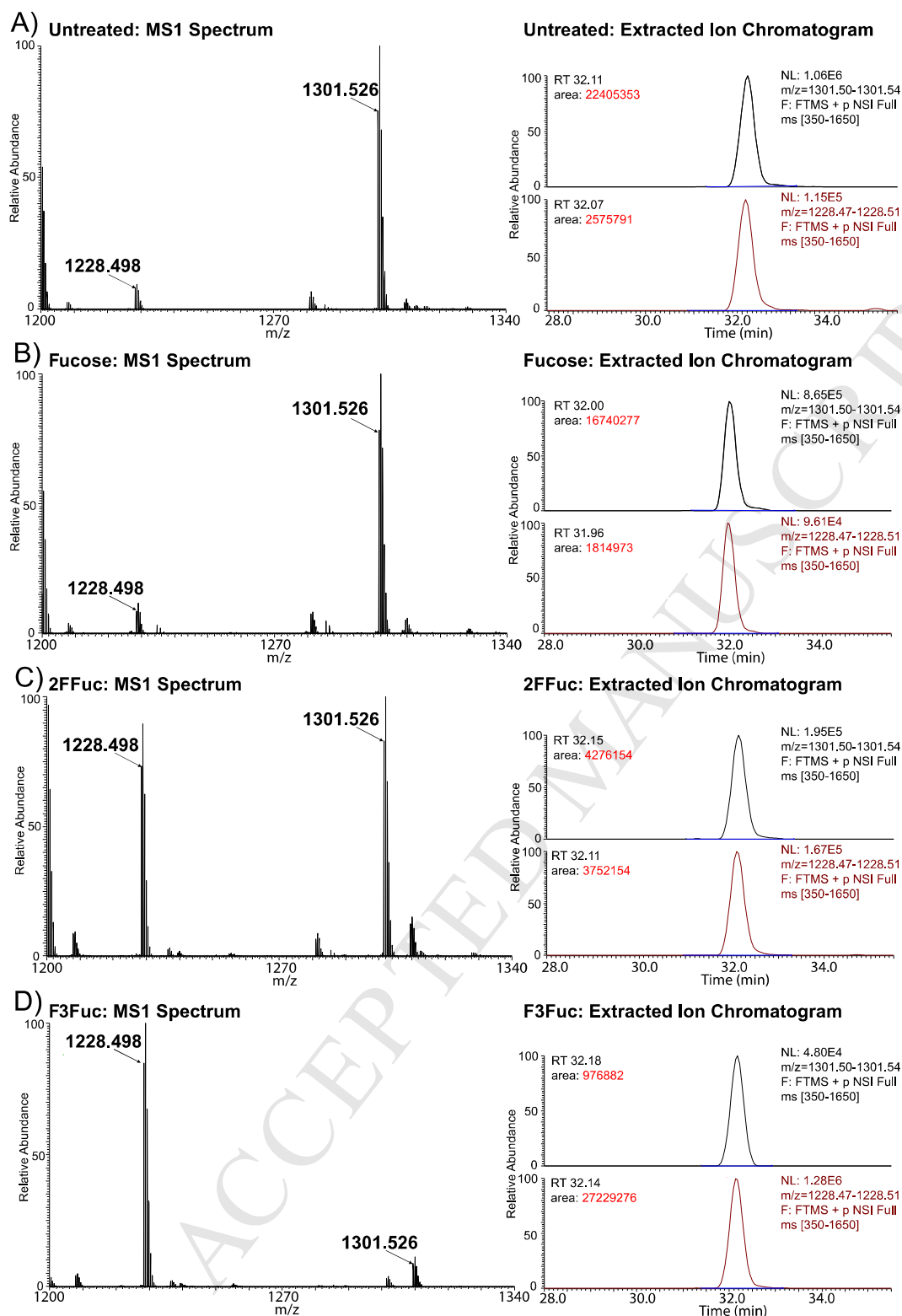


Figure 3. Mass spectra and extracted ion chromatograms for HexNAc₂Man₃GlcNAc₂ and HexNAc₂Man₃GlcNAc₂dHex glycoforms of the ¹⁷⁰EEQFNSTFR¹⁷⁸ peptide. The MS1 spectrum of the doubly charged forms of HexNAc₂Man₃GlcNAc₂ (m/z : 1228.50) and HexNAc₂Man₃GlcNAc₂dHex (m/z : 1301.53), as well as extracted ion chromatograms of the denoted

ions are shown for IgG1 purified from A) untreated; B) Fuc-treated; C) 2FFuc-treated and D) F3Fuc-treated hybridoma cell lines.

4. Experimental

4.1. General methods

All chemical reagents were purchased from Sigma-Aldrich at >95% purity and used without further purification, unless otherwise stated. All reactions were conducted under a N₂ atmosphere, unless otherwise stated, and monitored by thin layer chromatography (TLC) using aluminium backed Merck Silica Gel 60 F₂₅₄ sheets. TLC plates were visualised with UV light (254 nm) and developed using 5% H₂SO₄ in EtOH, KMnO₄ solution, or ceric ammonium molybdate solution, with heating as necessary. Column chromatography was performed on RediSep[®] Rf silica columns using a CombiFlash[®] Rf purification system (Teledyne Isco) with variable UV detection. ¹H, ¹³C and ¹⁹F NMR spectra were recorded using a 500 MHz instrument. The chemical shift (δ) of all resonances is reported in parts per million (ppm) relative to tetramethylsilane (δ = 0 ppm), with coupling constants (J) provided in Hz. All spectra are calibrated to their residual solvent peaks: CDCl₃ (¹H δ 7.26 ppm, ¹³C δ 77.16 ppm), (CD₃)₂CO (¹H δ 2.05 ppm, ¹³C δ 29.84 ppm), CD₃OD (¹H δ 3.31 ppm, ¹³C δ 49.00 ppm) and D₂O (¹H δ 4.79 ppm, ¹³C calibrated by spiking sample with 1% CD₃OD). High-resolution mass spectrometry (HRMS) was performed on an Agilent 1290 infinity 6224 TOF LCMS using an RRHT 2.1×50 mm (1.8 μ m) C18 column (LC: gradient over 5 min with the flow rate of 0.5 ml min⁻¹, MS: gas temp. 325°C, drying gas 11 l min⁻¹, nebulizer 45 psig, fragmentor 125 V). Melting points were obtained using a hot-stage microscope.

4.2. Synthetic Procedures

4.2.1. 1-Deoxy-3,4:6,7-di-*O*-isopropylidene-1,1,1-trifluoro- β -D-manno-hept-2-ulofuranose (**3**)

Tetrabutylammonium fluoride (1.00 M in THF, 58.6 ml, 58.6 mmol) was added drop-wise to a solution of 2,3:5,6-di-*O*-isopropylidene-D-mannonolactone **2**[18, 19] (13.8 g, 53.3 mmol) and TMSCF₃ (9.46 ml, 9.10 g, 64.0 mmol) in anhydrous THF (150 ml) at 0°C. The mixture was warmed to RT, stirred (12 h), diluted with EtOAc (100 ml) and washed with brine (3×100 ml). The organic phase was dried (MgSO₄), filtered and concentrated under reduced pressure. The residue was purified by recrystallization (EtOAc/cHex) to afford the hemiketal **5** (16.6 g, 95%) as colourless cubes. This single anomer underwent slow mutarotation in solution. ¹H NMR (500 MHz, CDCl₃) δ 1.32 (3H, s, CH₃), 1.37 (3H, s, CH₃), 1.43 (3H, s, CH₃), 1.48 (3H, s, CH₃), 4.03 (1H, ABX, $J_{7a,6}$ = 6.2, $J_{7a,7b}$ = 9.0 Hz, H_{7a}), 4.08 (1H, ABX, $J_{7b,6}$ = 4.2 Hz, H_{7b}), 4.13 (1H, m, H₅), 4.15 (1H, m, OH), 4.46 (1H, ddd, $J_{6,5}$ = 7.3 Hz, H₆), 4.71 (1H, d, $J_{3,4}$ = 5.9 Hz, H₃), 4.88 (1H, dd, $J_{4,5}$ = 3.7 Hz, H₄); ¹³C

NMR (125.7 MHz, CDCl₃) δ 24.4, 25.2, 25.4, 26.8 (4C, CH₃), 66.3 (C7), 72.9 (C6), 79.8 (C4), 80.4 (C5), 85.2 (C3), 102.0 (q, $J_{\text{C1-F}} = 32.6$ Hz, CCF₃), 109.66, 114.22 (2C, C(CH₃)₂), 121.58 (1C, q, $J_{\text{C1-F}} = 284.2$ Hz, CF₃); ¹⁹F NMR (470.4 MHz, CDCl₃) δ -141.48 (CF₃), HRMS-ESI m/z [M + H]⁺ calc'd for C₁₃H₁₉F₃O₆: 329.1206, found: 329.1212.

4.2.2. 2,5-Di-O-benzoyl-1-deoxy-3,4:6,7-di-O-isopropylidene-1,1,1-trifluoro-D-glycero-D-galactohexitol and 2,5-di-O-benzoyl-1-deoxy-3,4:6,7-di-O-isopropylidene-1,1,1-trifluoro-D-glycero-D-galactohexitol (**4**)

Sodium borohydride (6.62 g, 175 mmol) was added portion-wise to a solution of the hemiketal **3** (9.59 g, 29.2 mmol) in EtOH (100 ml) at 0 °C. The reaction mixture was refluxed at 70°C (12 h), chilled to 0°C, and quenched by the drop-wise addition of sat. NH₄Cl. The EtOH was removed under reduced pressure and the mixture partitioned between H₂O (200 ml) and EtOAc (100 ml). The organic phase was washed with sat. NaHCO₃ (100 ml) and brine (100 ml), dried (MgSO₄), filtered and concentrated under reduced pressure. Benzoyl chloride (17.0 ml, 146 mmol) was added drop-wise to a solution of the residue, pyridine (9.42 ml, 117 mmol) and DMAP (5 mg) in CH₂Cl₂ (150 ml) at 0°C and the mixture stirred at RT (16 h). *N,N*-Diethylethylenediamine (13.3 ml, 95 mmol) was added and the mixture stirred at RT (1 h). The mixture was diluted with CH₂Cl₂ (50 ml), washed with 1 M HCl (2×200 ml), sat. NaHCO₃ (200 ml) and brine (100 ml). The organic phase was dried (MgSO₄), filtered and concentrated under reduced pressure. The residue was purified by column chromatography (PhMe/EtOAc; 1:0–9:1) to afford **4** (12.1 g, 80%) as a colourless glass containing a 4:1 mixture of diastereomers. ¹H NMR (500 MHz, CDCl₃) δ 1.39 (3H, s, CH₃), 1.39 (3H, s, CH₃), 1.50 (3H, s, CH₃), 1.53 (3H, s, CH₃), 3.98 (1H, ABX, $J_{7a,6} = 7.2$, $J_{7a,7b} = 8.6$ Hz, H7_a), 4.12 (1H, ABX, $J_{7b,6} = 6.0$, Hz, H7_b), 4.26-4.32 (1H, m, H6), 4.61 (1H, t, $J_{4,5} = 6.6$, $J_{4,3} = 6.3$ Hz, H4), 4.73 (1H, dd, $J_{3,2} = 4.2$ Hz, H3), 5.54 (1H, dd, $J_{5,6} = 8.0$ Hz, H5), 6.15-6.23 (1H, m, H2), 7.38-7.47 (4H, m, Ar), 7.52-7.60 (2H, m, Ar), 7.95-7.99 (2H, m, Ar), 8.05-8.10 (2H, m, Ar); ¹³C NMR (500 MHz, CDCl₃) δ 25.52, 25.80, 26.18, 26.37 (4C, CH₃), 67.87 (C7), 68.12 (C2), 71.07 (C5), 73.53 (C3), 75.81 (C6), 77.31 (C4), 109.94, 110.54 (2C, C(CH₃)₂), 124.71 (CF₃), 128.44, 128.53, 130.03, 130.37, 133.21, 133.60 (12C, Ar), 164.95, 165.43 (2C, C=O); ¹⁹F NMR (500 MHz, CDCl₃) δ -136.64 (CF₃), -136.74 (CF₃), HRMS-ESI m/z [M + Na]⁺ calcd for C₂₇H₂₉F₃O₈: 561.1707, found: 561.1724

4.2.3. 2,5-Di-O-benzoyl-1-deoxy-1,1,1-trifluoro-D-glycero-D-galactohexitol (**5b**)

Water (1 ml) was added to a solution of the ketal **4** (450 mg, 0.836 mmol) in AcOH (4 ml) and the solution heated at 90°C (2.5 h). The solvent was removed under reduced pressure, co-evaporated with PhMe (2×5 ml) and the residue recrystallized from hot MeOH/CHCl₃ to give **5b** (257 mg, 67%)

as colourless crystals. ¹H NMR (500 MHz, (CD₃)₂CO) δ 3.59 (1H, ABX, H7_a), 3.67 (1H, ABX, H7_b), 3.82 (1H, t, *J*_{7,OH} = 5.8 Hz, OH), 4.09-4.19 (3H, m, H3, H4, H6), 4.38 (1H, d, *J*_{6,OH} = 5.7 Hz, OH), 4.72 (1H, d, *J*_{4,OH} = 6.3 Hz, OH), 4.81 (1H, d, *J*_{3,OH} = 8.4 Hz, OH), 5.49 (1H, d, *J*_{5,6} = 7.1 Hz, H5), 6.10 (1H, q, *J*_{2,3} = 7.5 Hz H2), 7.52-7.62 (4H, m, Ar), 7.65-7.70 (1H, m, Ar), 7.70-7.76 (1H, m, Ar), 8.10-8.13 (2H, m, Ar), 8.17-8.20 (2H, m, Ar); ¹³C NMR (500 MHz, (CD₃)₂CO) δ 64.06 (C7), 69.16, 69.91 (C3, C4), 69.74 (1C, q, *J*_{C1-CF3} = 30.4 Hz, CCF₃), 72.00 (C6), 73.49 (C5), 125.28 (1C, q, *J*_{C-F} = 281.5 Hz, CF₃), 129.44, 129.64, 130.59, 130.87, 134.20, 134.79, (6C, Ar) 165.32, 166.96 (2C, C=O); ¹⁹F NMR (500 MHz, (CD₃)₂CO) δ -136.18 (CF₃), HRMS-ESI *m/z* [2M + Na]⁺ calcd for C₂₁H₂₁F₃O₈: 939.2269, found: 939.2277

214

4.2.4. 3,4,6,7-Tetra-*O*-acetyl-2,5-di-*O*-benzoyl-1-deoxy-1,1,1-trifluoro-*D*-glycero-*D*-galacto-heptitol (6)

Acetic anhydride (0.12 ml, 1.23 mmol) was added to solution of tetraol **5b** (94 mg, 0.21 mmol), pyridine (0.2 ml, 2.46 mmol) and DMAP (5 mg) in CH₂Cl₂ (5 ml) and the mixture stirred at RT (16 h). Methanol (0.5 ml) was added drop-wise and the mixture stirred at RT (1 h). The mixture was diluted with CH₂Cl₂ (10 ml) and the organic layer washed with 1 M HCl (15 ml), H₂O (15 ml), sat. NaHCO₃ (15 ml), dried (MgSO₄), filtered and concentrated under reduced pressure. The residue was purified by column chromatography (cHex/EtOAc; 1:0–1:1) to afford tetracetate **6** (114 mg, 0.18 mmol, 89%) as a colourless crystalline solid. Crystals suitable for X-ray diffraction experiments were obtained by recrystallization from EtOAc/cHex. ¹H NMR (500 MHz, CDCl₃) δ 1.93 (3H, s, CH₃), 1.95 (3H, s, CH₃), 2.08 (3H, s, CH₃), 2.09 (3H, s, CH₃), 4.02 (1H, dd, *J*_{7a,6} = 5.2, *J*_{7a,7b} = 12.5 Hz, H7_a), 4.29 (1H, dd, *J*_{7b,6} = 3.3 Hz, H7_b), 5.12 (1H, ddd, *J*_{6,5} = 8.4 Hz, H6), 5.53 (1H, dd, *J*_{5,4} = 2.2 Hz, H5), 5.66-5.78 (3H, m, H2, H3, H4), 7.45-7.51 (4H, m, Ar), 7.58-7.65 (2H, m, Ar), 8.02-8.06 (2H, m, Ar), 8.07-8.15 (2H, m, Ar); ¹³C NMR (500 MHz, CDCl₃) δ 20.62, 20.65, 20.65, 20.81 (CH₃), 61.97 (C7), 65.84, 68.03 (C3, C4), 66.86 (q, C2), 67.25 (C5), 68.39 (C6), 119.48, 121.72, 123.97, 126.22 (CF₃), 128.74, 128.74, 129.99, 130.24, 133.86, 134.13 (12C, Ar), 164.56, 165.28 (2C, C=O), 168.94, 169.54, 169.92, 170.52 (4C, OCCH₃); ¹⁹F NMR (500 MHz, CDCl₃) δ -74.12 (CF₃), -73.97 (CF₃), -73.14 (CF₃), HRMS-ESI *m/z* [M + Na]⁺ calcd for C₂₉H₂₉F₃O₁₂: 649.1503, found: 649.1510

234

4.2.5. 2,5-Di-*O*-benzoyl-6,6,6-trifluoro-*L*-fucofuranose (7)

A solution of NaIO₄ (119.1 mg, 0.557 mmol) in H₂O (0.5 ml) was added drop-wise to a solution of tetraol **5b** (232mg, 0.51mmol) in MeOH (6 ml) at 0°C and the mixture stirred at this temperature (2 h). Solvent was removed under reduced pressure and the residue co-evaporated with PhMe (2×5 ml)

before column chromatography (cHex/EtOAc; 1:0–1:1) to afford the hemiacetal **7** (213 mg, 0.50 mmol, 97%) as a colourless glass. HRMS-ESI m/z $[2M + Na]^+$ calcd for $C_{20}H_{17}F_3O_7$: 875.1745, found: 875.1752

4.2.6. 6,6,6-Trifluoro-L-fucose, F3Fuc (**1**)

Sodium methoxide in MeOH (100 μ l, 25 wt. %) was added to a solution of the benzoate **7** (2.14 g, 5.03 mmol) in MeOH (20 ml) and the solution stirred at RT (1 h). The solution was neutralized with Amberlite[®] IR-120 (H^+ form) resin, filtered and concentrated under reduced pressure. The residue was purified by column chromatography (EtOAc/MeOH; 1:0–9:1) to afford 6,6,6-trifluoro-L-fucose **1** (54.0 mg, 0.25 mmol, 92%) as a colourless glass. 1H NMR and ^{13}C NMR data were commensurate with those previously reported.[16] HRMS-ESI m/z $[2M + Na]^+$ calcd for $C_6H_9F_3O_5$: 459.0696, found: 459.0743

4.3. X-ray crystallography

Single crystals of **6** were grown using the vapour diffusion method (EtOAc, hexanes). Intensity data were collected with an Oxford Diffraction SuperNova CCD diffractometer using Cu-K α radiation. The temperature during data collection was maintained at 200.0(1) K using an Oxford Cryosystems cooling device. The structure was solved by direct methods and difference Fourier synthesis.[21] Thermal ellipsoid plots were generated using the program ORTEP-3[22] integrated within the WINGX[23] suite of programs.

Crystal data for **6**; $C_{41}H_{53}F_3O_{12}$, $M = 794.83$, $T = 200.0$ K, $\lambda = 1.54184$, Monoclinic, space group C2, $a = 15.9117(3)$, $b = 13.9641(2)$, $c = 20.4533(4)$ Å, $\beta = 108.969(2)^\circ$ $V = 4297.77(14)$ Å³, $Z = 4$, $D_c = 1.228$ mg M^{-3} $\mu(Mo-K\alpha) 0.825$ mm⁻¹, $F(000) = 1688$, crystal size 0.65 x 0.32 x 0.20 mm³, 16517 reflections measured, $\theta_{max} 77.08^\circ$ 5919 independent reflections [$R(int) = 0.0209$], the final R was 0.0444 [$I > 2\sigma(I)$] and $wR(F^2)$ was 0.1356 (all data), Absolute Structure Parameter -0.02(7).

4.4. Cell culture and protein purification

4.4.1. Hybridoma culture

T25 culture flasks containing 10 ml SFM + 1% FBS and either L-fucose, 2-deoxy-2-fluoro-L-fucose or 6,6,6-trifluoro-L-fucose (10 mM) were seeded with murine hybridoma cells (1×10^6 cells/ml) and grown to 90% confluence at 37°C under an atmosphere of 5% CO₂. The cultures were centrifuged ($250 \times g$, 10 min) and the supernatant collected, filtered (0.45 μ m), and frozen until further use.

4.4.2. IgG purification

Protein G Sepharose beads (200 μ l of a 50% suspension) were added to hybridoma culture supernatant (10 ml) and the mixture nutated (4°C, 2 h). The beads were collected by centrifugation (500 \times g, 2 min, 4°C), transferred to a spin column (Pierce, 1 ml) and washed with 2 \times 500 μ l TBS-T (50 mM Tris, 150 mM NaCl, 0.1% Triton X-100, pH 7.5) and 2 \times 500 μ l TBS (50 mM Tris, 150 mM NaCl, pH 7.5). The IgG was eluted from the beads using 200 μ l citrate buffer (50 mM citric acid, pH 3.0) and the sample quickly neutralized using 35 μ l Tris buffer (1 M Tris, pH 8). This process was repeated three more times using the same hybridoma culture and protein G beads. The combined IgG samples were concentrated and buffer exchanged into TBS using a centrifugal filter unit (Amicon, 10K NMWL).

4.5. Protein mass spectrometry

4.5.1. Trypsin digestion of IgG1

Affinity isolated IgG samples were separated using SDS-PAGE, fixed and visualized with Coomassie G-250 according to the protocol of Kang *et al* [24]. Heavy chain bands were excised and destained in a 50:50 solution of 50 mM NH_4HCO_3 / 100% EtOH for 20 min at r.t. with shaking (750 rpm). Destained samples were washed with 100% EtOH, vacuum-dried for 20 min and rehydrated in 50 mM NH_4HCO_3 with 10 mM DTT. Disulfide reduction was carried out for 60 min at 56°C with shaking. The reducing buffer was then removed and the gel bands washed twice in 100% EtOH for 10 min to remove residual DTT. These samples were directly alkylated with 55 mM iodoacetamide in 50 mM NH_4HCO_3 in the dark for 45 min at r.t. Alkylated samples were washed twice with 100% EtOH and vacuum-dried, then rehydrated with 40 mM NH_4HCO_3 containing 12 ng μl^{-1} trypsin (Promega, Madison WI) and kept at 4°C for 1 h. Excess trypsin solution was removed, gel pieces were covered in 40 mM NH_4HCO_3 and incubated overnight at 37°C. The supernatant, containing peptides of interest, were concentrated and desalted using C_{18} stage tips [25, 26] before analysis by LC-MS.

4.5.2. Identification of glycopeptides using reversed phase LC-MS, CID MS-MS and HCD MS-MS

Desalted tryptic peptides were resuspend in Buffer A* (0.1% trifluoroacetic acid, 2% MeCN) and separated using a two-column chromatography set up composed of a PepMap100 C_{18} 20mm \times 75 μ m trap and a PepMap C_{18} 500 mm \times 75 μ m analytical columns (Thermo Scientific, San Jose CA). Samples were concentrated onto the trap column at 5 $\mu\text{l min}^{-1}$ for 5 min with Buffer A (0.1% formic acid, 2% MeCN) and infused into an LTQ-Orbitrap Elite (Thermo Scientific, San Jose CA) at 300 nl min^{-1} via the analytical column using an Dionex Ultimate 3000 UPLC (Thermo Scientific). A

90 min gradient was run from 2% Buffer B (0.1% formic acid, 80% MeCN) to 32% B over 51 min, then from 32% B to 40% B in the next 5 min, then increased to 100% B over 2 min period, held at 100% B for 2.5 min, and then dropped to 0% B for another 20 min. The LTQ-Orbitrap Elite was operated in a data-dependent mode automatically switching between MS, CID MS-MS and HCD MS-MS as previously described.[27]

4.5.3. Identification and annotation of observed glycopeptides

Raw files were processed manually to identify possible glycopeptides by examining all scans containing the diagnostic HexNAc oxonium 204.08 m/z ion. All scans containing these ions were manually inspected and identified as possible glycopeptides based on the presence of the deglycosylated peptide ion, corresponding to predicted glycopeptides of the *Mus musculus* IgG1 heavy chain (uniprot number: P01868). Potential glycan compositions were determined using the GlycoMod tool, (<http://web.expasy.org/glycomod/>), and composition confirmed by manual MS/MS assignment. Examples of all identified glycopeptides are provided within Figure S1, with glycopeptides annotated according to Domon and Costello and carbohydrate nomenclature of the Consortium for Functional Glycomics (<http://www.functionalglycomics.org/>).[28]

4.5.4. Comparison of glycoforms abundance

Relative fucosylation levels were determined using the ratio of the area under the curve for the monoisotopic peak of identified deoxyhexose-modified glycopeptides and unmodified versions of the same peptide similar to the previously reported method of Schulz and Aeibi for the determination of glycosylation occupation rates.[29] The areas under the curve for the monoisotopic peak were extracted using Xcalibur v2.2 and are provided within Figures S2–4.

Acknowledgement

The authors thank Kaye Wycherley and Paul Masendycz for providing the hybridoma cells lines used in this research. They also acknowledge support from the Australian Cancer Research Foundation, Victorian State Government Operational Infrastructure Support and Australian Government NHMRC IRIISS. This work was facilitated by a NHMRC project grant (APP1100164) awarded to NES. NCM and AJ were supported by an Australian Postgraduate Award, NES was supported by a NHMRC CJ Martin Fellowship (1037373) and EDG-B was supported by a VESKI Innovation Fellowship.

Supplementary data

Supplementary data related to this article can be found at ...

References

- [1] X.R. Jiang, A. Song, S. Bergelson, T. Arroll, B. Parekh, K. May, S. Chung, R. Strouse, A. Mire-Sluis, M. Schenerman, *Nature reviews. Drug discovery*, 10 (2011) 101-111.
- [2] J.S. Orange, *Nature reviews. Immunology*, 8 (2008) 713-725.
- [3] C. Ferrara, S. Grau, C. Jager, P. Sondermann, P. Brunker, I. Waldhauer, M. Hennig, A. Ruf, A.C. Rufer, M. Stihle, P. Umana, J. Benz, *Proceedings of the National Academy of Sciences of the United States of America*, 108 (2011) 12669-12674.
- [4] A. Okazaki, E. Shoji-Hosaka, K. Nakamura, M. Wakitani, K. Uchida, S. Kakita, K. Tsumoto, I. Kumagai, K. Shitara, *Journal of molecular biology*, 336 (2004) 1239-1249.
- [5] R. Niwa, M. Sakurada, Y. Kobayashi, A. Uehara, K. Matsushima, R. Ueda, K. Nakamura, K. Shitara, *Clinical cancer research : an official journal of the American Association for Cancer Research*, 11 (2005) 2327-2336.
- [6] R.L. Shields, J. Lai, R. Keck, L.Y. O'Connell, K. Hong, Y.G. Meng, S.H. Weikert, L.G. Presta, *The Journal of biological chemistry*, 277 (2002) 26733-26740.
- [7] R. Niwa, S. Hatanaka, E. Shoji-Hosaka, M. Sakurada, Y. Kobayashi, A. Uehara, H. Yokoi, K. Nakamura, K. Shitara, *Clinical cancer research : an official journal of the American Association for Cancer Research*, 10 (2004) 6248-6255.
- [8] S. Iida, H. Misaka, M. Inoue, M. Shibata, R. Nakano, N. Yamane-Ohnuki, M. Wakitani, K. Yano, K. Shitara, M. Satoh, *Clinical cancer research : an official journal of the American Association for Cancer Research*, 12 (2006) 2879-2887.
- [9] J.M. Subramaniam, G. Whiteside, K. McKeage, J.C. Croxtall, *Drugs*, 72 (2012) 1293-1298.
- [10] N.M. Okeley, S.C. Alley, M.E. Anderson, T.E. Boursalian, P.J. Burke, K.M. Emmerton, S.C. Jeffrey, K. Klussman, C.L. Law, D. Sussman, B.E. Toki, L. Westendorf, W. Zeng, X. Zhang, D.R. Benjamin, P.D. Senter, *Proceedings of the National Academy of Sciences of the United States of America*, 110 (2013) 5404-5409.
- [11] J.G. Allen, M. Mujacic, M.J. Frohn, A.J. Pickrell, P. Kodama, D. Bagal, T. San Miguel, E.A. Sickmier, S. Osgood, A. Swietlow, V. Li, J.B. Jordan, K.W. Kim, A.C. Rousseau, Y.J. Kim, S. Caille, M. Achmatowicz, O. Thiel, C.H. Fotsch, P. Reddy, J.D. McCarter, *ACS chemical biology*, 11 (2016) 2734-2743.
- [12] Y. Kizuka, M. Nakano, Y. Yamaguchi, K. Nakajima, R. Oka, K. Sato, C.-T. Ren, T.-L. Hsu, C.-H. Wong, N. Taniguchi, *Cell Chemical Biology*, 24 (2017) 1467-1478.e1465.

- 373 [13] E. Al-Shareffi, J.L. Chaubard, C. Leonhard-Melief, S.K. Wang, C.H. Wong, R.S. Haltiwanger,
374 Glycobiology, 23 (2013) 188-198.
- 375 [14] T.L. Hsu, S.R. Hanson, K. Kishikawa, S.K. Wang, M. Sawa, C.H. Wong, Proceedings of the
376 National Academy of Sciences of the United States of America, 104 (2007) 2614-2619.
- 377 [15] R.C. Bansal, B. Dean, S.-i. Hakomori, T. Toyokuni, Journal of the Chemical Society, Chemical
378 Communications, (1991) 796-798.
- 379 [16] M.M. Achmatowicz, J.G. Allen, M.M. Bio, M.D. Bartberger, C.J. Borths, J.T. Colyer, R.D.
380 Crockett, T.-L. Hwang, J.N. Koek, S.A. Osgood, S.W. Roberts, A. Swietlow, O.R. Thiel, S. Caille,
381 The Journal of Organic Chemistry, 81 (2016) 4736-4743.
- 382 [17] J.P. Gesson, J.C. Jacquesy, M. Mondon, P. Petit, Tetrahedron Letters, 33 (1992) 3637-3640.
- 383 [18] K.P.R. Kartha, Tetrahedron Letters, 27 (1986) 3415-3416.
- 384 [19] M.B. Fusaro, V. Chagnault, S. Josse, D. Postel, ChemInform, 44 (2013).
- 385 [20] J.H. Nam, F. Zhang, M. Ermonval, R.J. Linhardt, S.T. Sharfstein, Biotechnology and
386 bioengineering, 100 (2008) 1178-1192.
- 387 [21] G. Sheldrick, Acta Crystallographica Section C, 71 (2015) 3-8.
- 388 [22] L. Farrugia, Journal of Applied Crystallography, 30 (1997) 565.
- 389 [23] L. Farrugia, Journal of Applied Crystallography, 32 (1999) 837-838.
- 390 [24] D. Kang, Y.S. Gho, M. Suh, C. Kang, Bull. Korean Chem. Soc., 23 (2002) 2.
- 391 [25] Y. Ishihama, J. Rappsilber, M. Mann, J Proteome Res, 5 (2006) 988-994.
- 392 [26] J. Rappsilber, M. Mann, Y. Ishihama, Nature protocols, 2 (2007) 1896-1906.
- 393 [27] N.E. Scott, B.L. Parker, A.M. Connolly, J. Paulech, A.V. Edwards, B. Crossett, L. Falconer, D.
394 Kolarich, S.P. Djordjevic, P. Hojrup, N.H. Packer, M.R. Larsen, S.J. Cordwell, Molecular & cellular
395 proteomics : MCP, 10 (2011) M000031-mcp000201.
- 396 [28] B. Domon, C.E. Costello, Glycoconjugate Journal, 5 (1988) 397-409.
- 397 [29] B.L. Schulz, M. Aebersold, Mol Cell Proteomics, 8 (2009) 357-364.
- 398

Highlights

- 6,6,6-Trifluoro-L-fucose (F3Fuc) can be readily synthesised from D-mannose.
- F3Fuc is effective at blocking antibody fucosylation in hybridoma cell lines.
- F3Fuc is superior to other fucose mimics at blocking fucosylation in hybridoma cell lines.